



Assessment of the rock slope stability of Fushun West Open-pit Mine

Fei Zhang^{1,2,3} · Tianhong Yang⁴ · Lianchong Li⁴ · Jianqing Bu^{1,2} · Tianliang Wang^{1,2,3} · Ping Xiao⁵

Received: 18 December 2020 / Accepted: 1 July 2021 / Published online: 22 July 2021
© Saudi Society for Geosciences 2021

Abstract

The stability of the slope is directly related to the safety operation of the open-pit and the life safety of personnel. Effective evaluation of slope stability can reduce the loss caused by slope disasters such as the Fushun West Open-pit Mine. In recent years, some damage has occurred in the south slope of the mine. Therefore, a progressive research method combining the rock mass classification system, slope mass rating method and numerical method is proposed in this study to analyze the possible failure mode and deformation mechanism of the slope. The digital photogrammetry technology, borehole television technology, infrared scanning technology, and on-site monitoring are combined to obtain the relevant data needed for the method. Based on the rock mass characteristics and the survey on-site, the quality of the rock mass of the slope was evaluated through the rock mass classification system and the borehole TV technique. The slope mass classification system with essential adjustment factors considering the discontinuities and excavation methods are a feasible method to estimate rock slope stability. Thereafter the stability of the south slope was estimated by using the slope mass rating method. The results indicate that the stability of the slope is controlled by the weak bedding plane prone to planar failure. Additionally, the deformation mechanism and potential failure dimensions were analyzed through numerical method. Incorporating the empirical result with the numerical result indicates that the south slope is in limit equilibrium state and susceptible to failure along bedding planes. The resulting of the slope stability was validated using the monitoring data that obtained by the GPS devices in situ. According to the deformation characteristics, the corresponding reinforcement methods were established and achieved good result. The progressive methodology provides an effective way to assess the stability and serves for the formulation reinforcement scheme of the rock slope in the complex geological conditions.

Keywords High-steep slope · Slope stability · Rock mass rating · Slope mass rating · Planar failure slope

Responsible Editor: Murat Karakus

✉ Fei Zhang
zhangfei@stdu.edu.cn

- ¹ State Key Laboratory of Mechanical Behavior and System Safety of Traffic Engineering Structures, Shijiazhuang Tiedao University, Shijiazhuang 050043, China
- ² School of Civil Engineering, Shijiazhuang Tiedao University, Shijiazhuang 050043, China
- ³ Key Laboratory of Roads and Railway Engineering Safety Control (Shijiazhuang Tiedao University), Ministry of Education, Shijiazhuang 050043, China
- ⁴ Center of Rock Instability and Seismicity Research, School of Resources and Civil Engineering, Northeastern University, Shenyang 110819, Liaoning, China
- ⁵ West Open-pit Mine of Fushun Mining Group, Fushun 113001, Liaoning, China

Introduction

The rock slope stability is always a hot topic for researchers and engineers in the world. Therefore, many researchers proposed different methods to evaluate and analyze the stability of the slope in order to prevent disasters in advance and put forward the related management methods. As we know, the slope stability is the principal problem that the open-pit mine cares. With the continuous mining of the open-pit, the slope gradually becomes high and steep. Thus, the research on the stability of the slope is a meaningful thing for the mine and researchers. Fushun West Open-pit Mine is a large-scale open-pit with over 100 years of mining history (Fig. 1). Due to the excavation of the mine, the south slope has become a high-steep slope with the characteristics of large scale, strong weathering, and strong unloading. The slope failures in this area are caused by an interaction of a series of complex factors such as geological, geomorphological, and climatic. These factors are usually divided into two categories including

Fig. 1 The position and the overview of Fushun West Open-pit Mine



triggering factors and conditioning factors (Crozier 1986; Abuzied et al. 2016). The trigger factors cause the slope susceptible instability including excavation and rainfall. They play an important role in the slope instability of Fushun West Open-pit Mine. The conditioning factors lead to the slope susceptible to deformation containing lithology, discontinuities, slope et al. For the complex geological conditions, long-term of excavation and rainfall, a large deformation appeared since 2009. A great deal of cracks appeared on the slopes, the tension crack formed on the top of the slope, and a large heave can be observed on the bottom of the slope (Fig. 2). In the past few decades, several hundred millions of Chinese Yuan (CNY) was used to monitor and control the deformation of the slope. For the safety of the surrounding citizens and the manufacturing equipment, the relevant methods should be proposed to analyze the stability of the slope, and the corresponding reinforcement scheme should also be put forward as soon as possible. Hence, this study aims to develop a progressive method to estimate the rock slope stability considering the geological features, excavation methods, water condition, et al.

To evaluate the stability and deformation mechanism of rock slopes under complex geological conditions, the integration of different datasets and data analysis techniques are indispensable (Abuzied and Alrefaee 2019; Abuzied and Pradhan 2020). As we know, the slope stability in the engineering is affected by numerous factors. Therefore, it is hard

to directly identify the stability of the slope. The rock mass classification systems are based on the field experience and theory of previous scholars. It is a valid tool for estimating rock mass quality and properties, especially for the jointed rock mass (Santos et al. 2020; Rusydy et al. 2021). There are many rock mass classification systems to evaluate the rock stability such as the RQD system, Q system (Barton et al. 1974), the rock structure rating (RSR) (Wickham et al. 1972), the geological strength index (GSI) (Hoek et al. 2000), the rock mass rating (RMR) (Bieniawski 1973, 1989), and the mining rock mass rating (MRMR) (Laubscher 1990). Many scholars try to summarize the characteristics of slope stability and discuss the reliability of the classification methods. Some of the traditional classification systems lack of considering some triggering factors, for example, precipitation, that may normally induce the instability of the slope. Some of the classifications may not consider the specific factors of the slope condition. To overcome such shortcomings, the slope mass rating (SMR) (Bieniawski 1989) classification system has been proposed and developed (Pantelidis 2009, 2010). SMR method is an easy and helpful mean for slope stability estimation of jointed rock slopes (Huang et al. 2020; Singh et al. 2020). But the SMR method is too simple and is often used for a preliminary analysis of the slope stability (Tizzano et al. 2016). For a deep understanding of the deformation mechanism and failure process of the slopes, numerical methods are useful.

Fig. 2 The damage observed in situ



(a) the surface crack



(b) the tensile crack in the top of the slope



(c) the heave in the bottom of the slope



(d) some local region of planar failure

The slope stability always affects by different geological structure such as the bedding planes, faults, and joints. The discontinuities have significant effect on the stability of the

slope. A totally different type of failure mode may be caused by different combination of the discontinuities. Therefore, the discontinuities in the slope should be considered as a key

factor. The traditional classification system can only assess the effect of the discontinuities on the stability of the slope in general. It is hard to study the deformation mechanism and consider the detail conditions of the jointed slopes. The distinct element method (DEM) was developed and widely used to analyze the discontinuous issues in the geotechnical engineering. The Universal distinct element code (UDEC) is a convenient way to study the discontinuous problem of rock engineering such as the rock slope (Salmi and Hosseinzadeh 2015; Qi et al. 2016; Zheng et al. 2018), the tunnels (He et al. 2018; Farahmand and Diederichs 2021), mining engineering (Pinheiro et al. 2015; Liu et al. 2020), and hydraulic engineering (Zhang et al. 2015; Bhasin and Pabst 2015). The UDEC has achieved good results in analyzing the stability of the jointed slopes (Kalililo and Xia 2020; Zhao et al. 2020). The UDEC can reproduce the failure process by considering both the lithological and geological conditions. The slope failure is a dynamic process. Hence, the temporal evolution of the slope failure can help grasp past deformation characteristics and possibly forecast the deformation trend.

In this study, a progressive method is proposed to conduct an integrated assessment of the slope stability in Fushun West Open-pit Mine, with the aim of effectively and scientifically explaining the principal failure mechanisms potentially affecting the instability of the slope and raising the corresponding intervention measures. To achieve these goals, the RMR and SMR methods were quantitatively used to assess the stability of the rock slope. The distinct element model was established to investigate the progressive failure and possible deformation trend of the slope. Furthermore, it is more important to analyze the conditions leading to the instability in order to understand deeper insight into the failure process. Hence, this study adds the promising approach integrating the slope mass classification system and numerical method to evaluate the possible failure mode, deformation mechanism, failure probability, and possible failure trend of the rock slope. It can also assist the decision-makers to make a detailed reinforcement plan.

Study area and geological settings

The Fushun West Open-pit Mine is located in the north-east of China, 800 kilometers from the capital Beijing. It locates at the center of Fushun city covering 14.2 km². The south slope of the open-pit belongs to the deep and large slope. The maximum height of the slope has researched 400m. The slope is 6.6km long from east to west and 4.4km wide from north to south. The slope stabilities have a tremendous influence on the safety of the surrounding buildings and the citizens near the mine. The north side of the open-pit is the main water system of Hunhe River in Fushun, flowing through the city

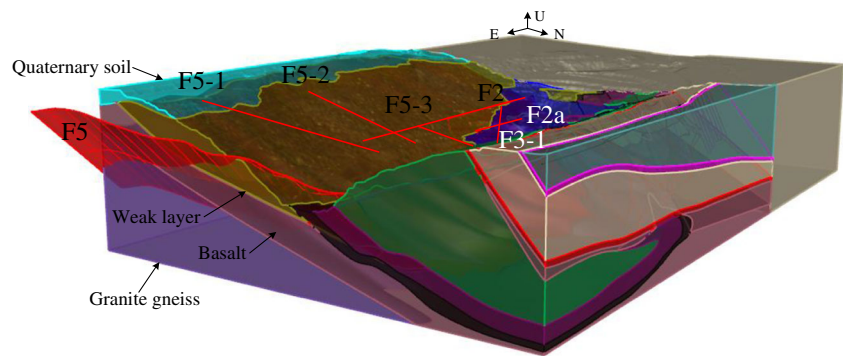
predominantly in the E–W direction. The south side of Qiantai Mountain is the Yangbai River flowing predominantly in the E–W directions. Some major rivers flow through the research area including Hunhe River, Yangbai River, and Gucheng River flowing predominantly in the E–W and N–S directions. The surrounding river plays an important role in the replenishment of the groundwater of the slopes, which leads to a culprit of the strength reduction of the slope rock mass.

The geomorphic type of the study area is hilly area with large undulations, and the open-pit area is a bench terrain formed by artificial transformation. Qiantai Mountain is located in the south of the open-pit with an elevation of +214m. Its north slope is connected with the south side of the pit. The south slope of the pit is a nonworking slope. From old to new, the strata in the study area are mainly: archean granite gneiss, cenozoic paleogene basalt and carbonaceous mudstone, quaternary alluvial strata, artificial accumulation layers, etc. Because of the excavation of the south slope, the Quaternary soil is stripped off and the basalt layer gradually exposed in the south slope, according to the weathering degree of the basalt; it is divided into three classes: strong weathered, medium weathered, and nonweathered. Excavation has also aggravated the instability of the slope. According to the geological drilling exploration, the bedding planes are included in the basalt layers.

The geological condition is complex due to the geological structures and strong unloading. Due to the influence of the main faults in the mining area, there are many longitudinal and transverse faults in the south slope, and there are many special anticline dips and folds. There are E–W fault structure (F2) and NW–SE fault structure (F5) in the central part and other faults such as F5-1 F5-2 F5-3, F2a, and F3-1 are also included in the south slope of the open-pit as shown in Fig. 3. In the past, small landslides in the study area were mostly related to faults and joints. Often, the borders on both sides of the landslide were joints and small north-south transverse faults, with a small drop, sometimes only 1–2m. For example, there are nearby W1200, W1050, and W300, and these small transverse faults are associated with the F5 fault in the study area.

Fushun has a semi humid continental monsoon climate in the north middle temperate zone. Affected by the cold air flow in Siberia and Mongolia Plateau and the warm and humid air flow in the Yellow Sea, Fushun is hot and rainy in summer and cold in winter. The annual average temperature is 5 ~ 6°C, the average temperature in January is -15 ~ -17°C, the minimum extreme temperature is -40.5°C, and the maximum extreme temperature is 40.3°C. The annual average rainfall is 808.1mm, mostly concentrated in July and August. The maximum daily rainfall is 180.3mm/d, and the maximum continuous rainfall is 963.5mm. The small landslides in the slope have a direct relationship with the rainfall.

Fig. 3 The geological condition of Fushun West Open-pit Mine



Data and methodology

A progressive method combining the slope mass classification and numerical method is considered in this study to identify the landslide susceptibility modes and analysis the deformation mechanism of the slope using specific characteristics of the joints, the spatial relationship between the joint and the slope, the water conditions, the excavation method of the slope. These data were achieved from the following resources:

- (1) The related joint parameters of the rock mass are mainly obtained in situ by using digital photogrammetry method. Then the stability of the slope can be comprehensively evaluated through the classification system and the numerical method.
- (2) The interior structure of the rock mass of the slope can be obtained by the borehole TV technique. The interior structure map of the rock mass can be used to access the quality of the rock mass that can't be observed directly in situ.
- (3) The infrared scanning technique was used to achieve the water distribution and delineate the water leakage position of the slope.
- (4) Field investigations with Global Positioning System (GPS) devices were performed on April 2013 to analysis the deformation characteristics and validate the numerical simulation results.
- (5) The input parameters during the numerical simulations were obtained from the laboratory tests, field observations, calculation, and literatures to further study the deformation mechanism of the slope.

Preparation of related data

In this study, some techniques and data provide important basis for slope stability analysis. The following paragraphs specifically explain the principles of these technologies and the sources of the data.

Acquisition of joint parameters

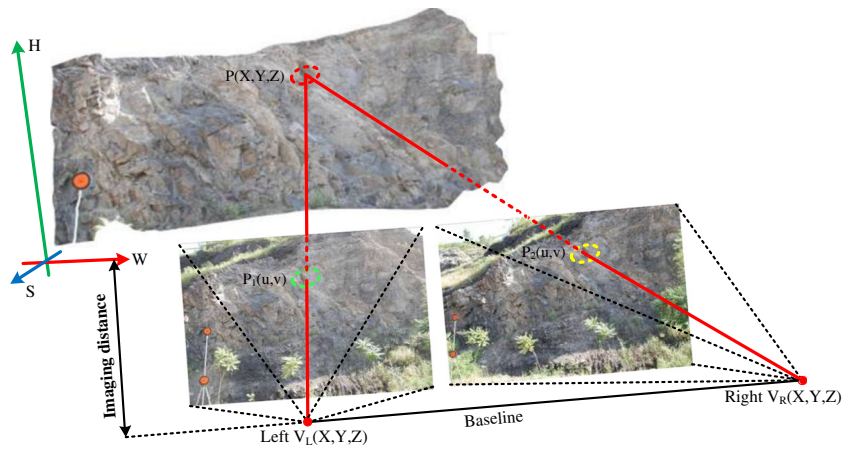
The advanced ShapeMetrix3D (Wang et al. 2013; Yang et al. 2015) technique of the three dimensional measurement systems for geometric parameters of rock mass is used to obtain the appointed area. The rock mass is captured from different angle and then the good image result is imported in the ShapeMetrix3D system. The real surface of the slope is synthesized from the left and right perspectives and labeled point. After the synthesis of the image, the joint in the surface of the slope is handled by a series of works. Therefore, a series of related parameters are obtained including the dip direction, dip angle, and the joint spacing. The principle of the ShapeMetrix3D system and the result of the identification of the joints are shown in Fig. 4.

The measurement of the joint is focused on three different regions of different benches. The position of the measurement area and the related position in this study are presented in Fig. 5. There are totally 2200 joints recognized by statistical means. The joints are summed up and analyzed by its related characteristics. Thus, the preferred structural plane are identified, the result is listed in Table 1. After summarizing and grouping the joints, the dominant joints can be identified. The dominant joint is $339^{\circ}\angle 34^{\circ}$ (J_1), $285^{\circ}\angle 52^{\circ}$ (J_2), and $106^{\circ}\angle 54^{\circ}$ (J_3) separately. The dominant joint sets can also be observed on-site as shown in Fig. 6. The joint parameters can be used to estimate the stability and understand the possible failure mode of the slope using the slope mass classification systems. The joint distribution and joint parameters can also provide basis for further analysis of numerical modeling. The data acquired by the digital photogrammetry technique is fully utilized for a deep understanding of the deformation mechanism and failure process of the slopes.

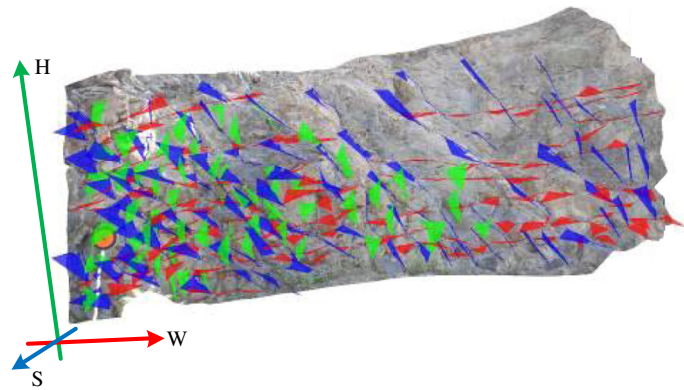
The map of the interior structure of the rock mass

The borehole TV technique is a technique which can provide a direct mean to observe the structure of interior rock mass on site. The borehole TV technique has the advantages of high-resolutions, high-precisions, and high well-logging working efficiency. It integrated the digital recording technique and

Fig. 4 The parameter of the discontinuities obtained by ShapeMetrix3D system



(a) the principle of the ShapeMetrix3D system



(b) the result of the identification of the joint

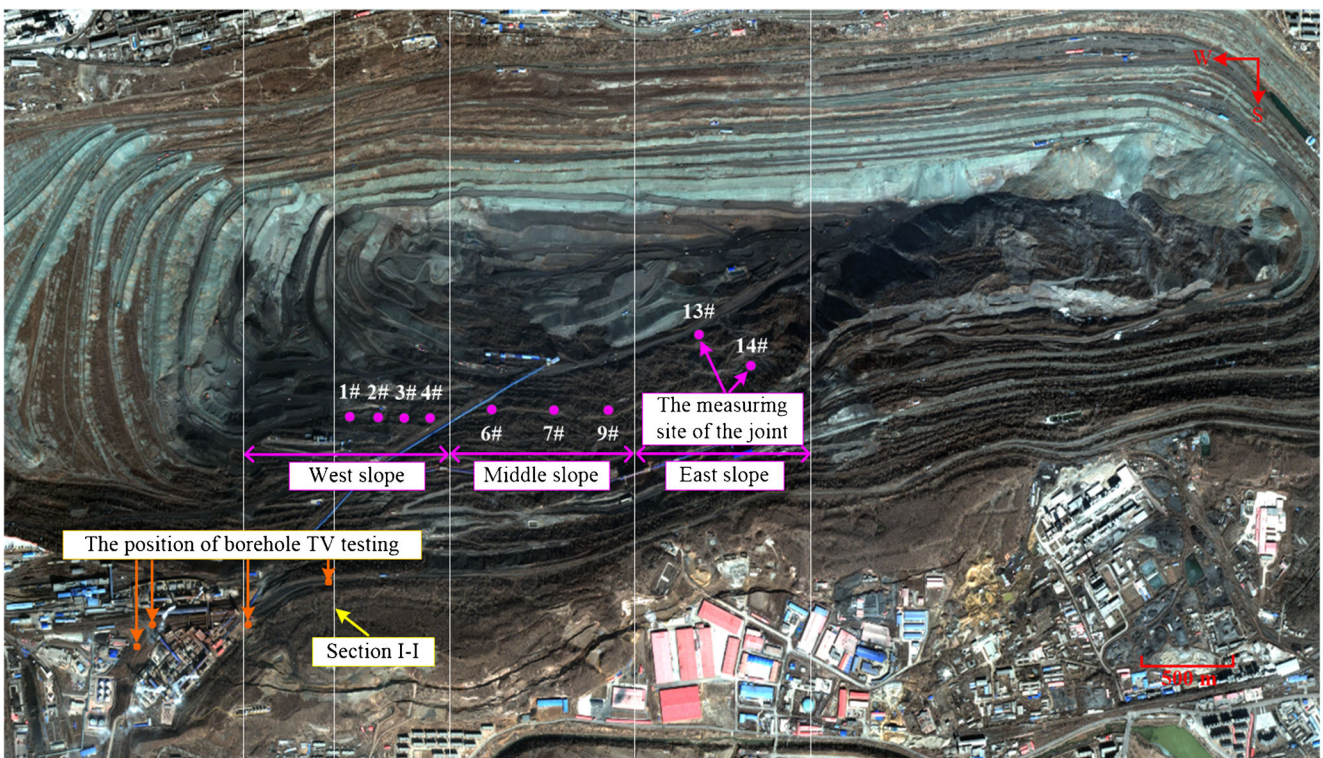


Fig. 5 The position of the discontinuities survey region and section I-I

Table 1 The in situ measurement of the discontinuities

The position of the survey point	ID	Dip direction/ Dip(°)	Joint number	Density(m ⁻¹)	Basic quality value	Grade		
+20m West slope	1	200.99/51.09	33	1.9203	438.58	III		
		337.23/30.70	16	2.2772				
		153.25/52.79	23	1.5109				
	2	91.05/31.05	42	0.7191			391.98	III
		233.05/80.97	61	0.3386				
		339.01/36.87	71	1.5918				
	3	16.32/36.18	175	2.7512			339.13	IV
		94.22/88.14	47	0.6029				
		200.69/68.97	45	1.4585				
	4	285.77/52.67	48	1.0146			436.42	III
		99.93/57.92	37	1.1721				
		279.78/39.78	37	1.612				
-20m Middle slope	6	101.72/74.36	112	0.7535	304.80	IV		
		250.56/57.11	77	0.4316				
	7	351.654/51.836	41	1.2882	404.97	III		
		278.57/37.93	85	1.1055				
	9	22.03/26.31	68	0.8808	392.26	III		
		336.71/60.32	35	1.7459				
-250m East slope	13	65.54/38.41	103	2.4341	266.58	IV		
		181.29/70.86	60	1.0073				
		292.795/76.869	38	0.6639				
-71m East slope	14	354.66/23.79	135	2.1675	410.64	III		
		239.95/78.81	74	1.0386				
		65.20/40.57	55	1.0730				
		312.92/33.80	124	1.4961				
		214.73/85.10	60	0.526				

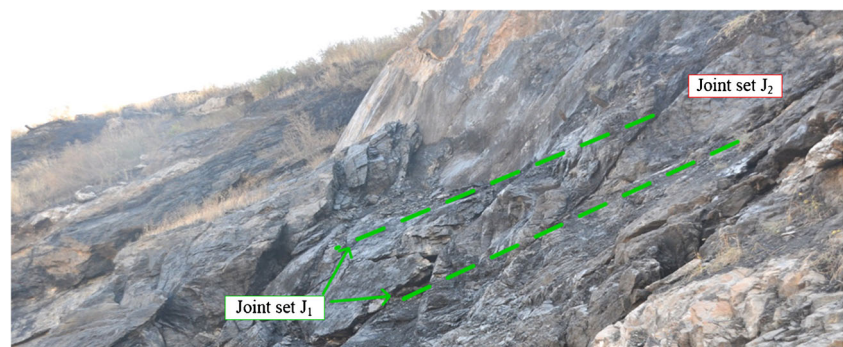
digital data processing technique. The borehole TV technique use the camera to capture the wall image of the borehole reflected by the conical mirror. Then the image information is transferred to the controller and the computer via the cable. The whole collection process is accessed by the image acquisition system. This system can further expand and merge the captured images and then record the images on the computers.

The borehole TV testing mainly performed in the south slope to study the unloading and quality of the rock mass and there are totally four test sites were selected (as shown in Fig. 5). A series of borehole TV testing results and digital

cores were obtained during the excavation and deformation of the slope. The result of the test map can be used to evaluate the damage and the quality of the rock mass as shown in Fig. 7.

The water leakage distribution map

Most landslides are commonly relating to the rainfall in Fushun West Open-pit Mine. When rainfall enters into the slope, it has a negative effect on the stability of the south slope. The infrared scanning technique can be used to identify the water distribution of the study area. As we know the

Fig. 6 The dominant joint set observed in situ

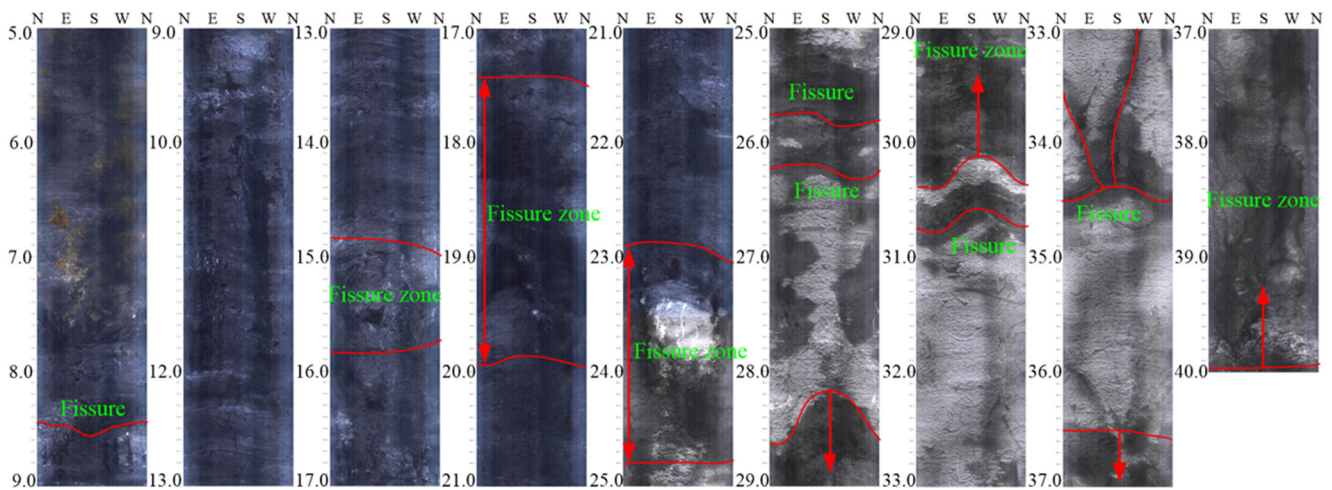


Fig. 7 The testing result of the borehole TV technique

objects in nature will absorb heat more or less, some of the heat will be radiated to the outside world in the form of infrared waves. The infrared scanning technique is a technology which can capture the infrared wave radiated by the creature. Thereafter the temperature field can be obtained by analyzing the infrared wave information. The infrared scanning technique mainly uses the infrared camera to monitor the temperature field information of the study area. Furthermore, the abnormal temperature area and the seepage area of the slope can be delineated. Hence, the water distribution map of the slope was obtained by using the infrared scanning technique. The monitoring result of the south slope in the open-pit is presented in Fig. 8. Thus, the leakage strip and other water distribution information of the slope can be achieved.

The monitoring data in situ

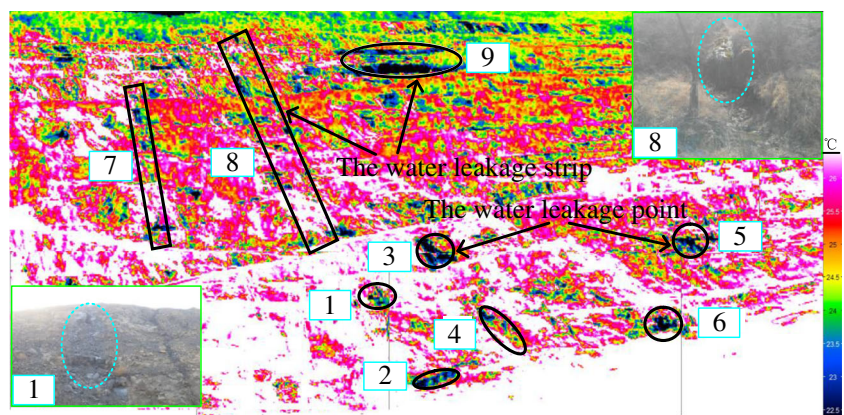
The monitoring data can directly reflect the deformation characteristics of the slope before and after the reinforcement. Three monitoring points on the top, middle, and bottom position of section I-I are selected to monitor the deformation characteristics of the slope. Field investigations with GPS

devices were performed and the data from April 2013 to October 2014 can be achieved as presented in Fig. 9. The slope deformation data can be divided into two stages according to the time of slope reinforcement. The GPS monitoring data can be used to study the whole deformation process of the slope before and after reinforcement and validate the result obtained by the numerical simulation.

The mechanical parameters

The researched area includes two rock layers and a weak layer. The mechanical parameters of related strata are of great significance to the numerical modeling in the study area. These parameters were obtained from the laboratory tests, field observations, and previous studies on the mechanical properties of rock masses in Fushun West Open-pit Mine (Yang et al. 2005; CCTEG 2013; Zhang et al. 2019). The normal and shear stiffness of the joints were estimated by the expressions in the reference (Itasca 2004). The input parameters during the numerical simulations are presented in Tables 2, 3 and 4 including the characteristics of the intact rock, soil and discontinuities (joint sets and bedding planes).

Fig. 8 The leakage point obtained by the infrared scanning technique



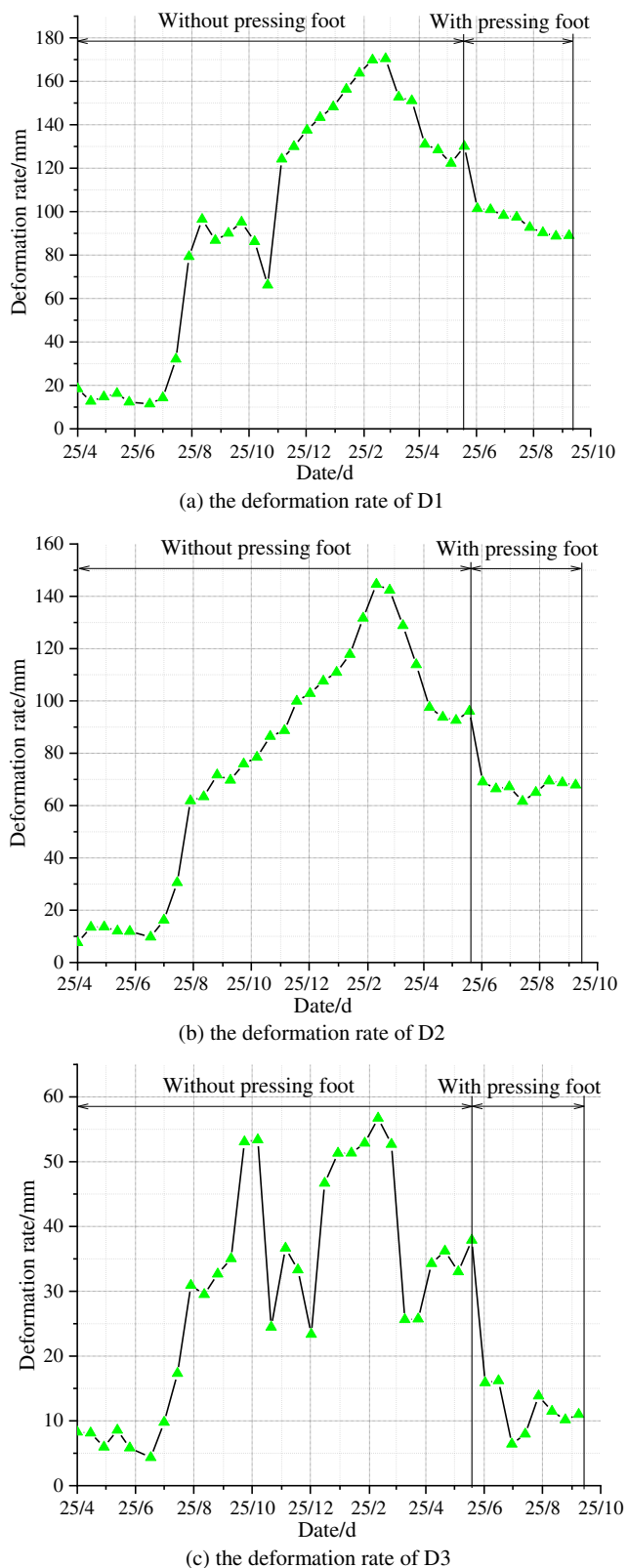


Fig. 9 The deformation rate monitored in-situ

The numerical modeling with the mechanical parameters can be used to analyze the deformation process of the slope.

The stability analysis methodology

The methodology used in this study is divided into three sections. First, the traditional classification system combining with the field survey and monitoring data were utilized to assess the quality of the rock mass. The evaluation of the rock mass can provide useful information for further analysis. Second, SMR method considering the excavation method was used access the possible failure modes of the slope. The empirical method can only consider a simplified failure mode and reinforcement, so numerical modeling was also established to study the deformation process, stress distribution, and yield status of the slope in detail. The numerical method using a discontinuum model can reflect the slope morphology and tectonic effect.

The rock mass classification

The rock mass quality is a main factor that affects the stability of the slope. The rock mass in good quality will reduce numerous sliding hazardous and the treatment cost of the slope. However, the rock mass in poor quality may induce a series of potential risks of the slope. Thus, the evaluation of the quality of the rock mass in the slope engineering is essential. The rock mass quality is influenced by a number of factors such as water effect, intact rock strength, discontinuities conditions, and the weathering degrees. Thus, the method was developed considering the spatial distribution characteristics of slope lithology and structure based on detail field survey and borehole TV technique.

As we know, some of the parameters are difficult or impossible to directly measure, thus, it is hard to assess the quality of the rock mass by accurate method. Therefore, many researchers propose a series of empirical methods to assess the quality of the rock mass in the engineering. In present study, the most commonly used empirical method to estimate the rock mass quality of the rock engineering project including the mining rock mass rating—MRMR (Laubscher 1990), the rock mass rating—RMR (Bieniawski et al. 1973), the geological strength index—GSI (Hoek et al. 2000), and the Q-system (Barton et al. 1974). The above mentioned methods have been developed to estimate the rock quality and stability of the rock engineering in both slope stability and the underground excavation.

In present study, the RMR system is widely applied in the rock mass quality estimation. It is used to estimate the different characteristics of the rock mass in quantization and then to evaluate the quality of the rock mass. The RMR system including the strength of the rock (I_1), the value of the index RQD (I_2), the spacing of the joints (I_3), the condition of discontinuities (I_4), and hydraulic conditions (I_5) totally five parameters.

Table 2 The parameters of the rock mass employed in the simulation

Item	Basalt	Weak layer	Granite gneiss	Backfill
Uniaxial compressive strength (MPa)	110	30	130	\
Young's modulus (MPa)	7000	100	8000	1200
Young's modulus for intact rock (GPa)	30	0.5	35	\
Tensile strength (MPa)	0.2	0.016	0.3	0.05
Poisson's ration	0.14	0.4	0.2	0.3
Cohesion (MPa)	0.14	0.018	0.15	0.1
Friction angle (°)	42	14	45	30
Bulk modulus (GPa)	2.71	0.06	3.33	0.57
Shear modulus (GPa)	3.07	0.04	3.33	0.46
Density (kg/m ³)	2800	2300	2800	1800

The values of related coefficients can be determined by the index listed in the reference (Bieniawski et al. 1973). The sum of each coefficient of RMR can describe the classification of the rock mass. Therefore, it can assess the stability of the rock mass and provide guidance for the engineering project.

According to the international standard for engineering classification of rock mass, the rock mass in the study area of the south slope is belong to the III grade and IV grade. The RQD (Rock Quality Designation) is calculated on the basis of a series of discontinuities parameters measured in situ (Barton et al. 1974). The distribution of water content of the slope can be obtained from the field survey and infrared scanning map. Additionally, some detailed works on the geological survey on-site have implemented. Thereafter the quality of the rock mass in the south slope can be evaluated.

The digital panoramic borehole TV technology can directly identify underground cracks, weak layers, and broken zones. Thus, the quality of the rock mass can be estimated during the excavation-unloading and deformation process of the slope. In recent years, the borehole TV technique has been widely applied in the fields of geotechnical engineering, such as the rock slope deformation (Chigira et al. 2013), the determination of the Excavation Damaged Zones (EDZs) in the underground excavation (Chen et al. 2015).

Table 3 The soil properties used in numerical modeling

Item	Quaternary soil
Density (kg/m ³)	1800
Friction angle (°)	18
Cohesion (kPa)	100
Bulk modulus (MPa/m)	13.89
Shear modulus (MPa/m)	8.93

Slope mass rating

In this part, the empirical method has performed to assess the probable failure modes of the south slope and provide guidance for the reinforcement of the slope. Bieniawski (1989) also proposed rating adjustments of different discontinuity orientations in rock slopes as presented in Table 5. The value of the discontinuity orientation adjustment coefficient is generally considered to be a negative number. The value is subtracted from the RMR value in order to estimate the stability of the slope. However, there is no clear definition of the classes mentioned in Table 5. Since the value of the adjustment factor is extremely high, it will involve uncertainty and lead to inaccurate results. Some studies show that the RMR classification method is not a successful method in evaluating the slope stability (Romana 1991; 1995a, b). If the RMR classification method is used as a slope estimation and design method solely, it will lead to errors in stability assessment due to the drawbacks of this method.

In order to evaluate the stability of the slope, Romana (1991) proposed the SMR based on the RMR classification system proposed by Bieniawski (1973). The SMR system considers the adjustment factors added or subtracted according to the specific jointing conditions and the used excavation method of the slope respectively. The SMR system has been widely applied in a great deal of slope engineering (Salmi and

Table 4 The parameters of discontinuities used in the analysis

Discontinuities	J ₁	J ₂	J ₃	Bedding plane
Cohesion (MPa)	0.0012	0.0014	0.0014	0.001
Friction angle (°)	26	28	28	18
Normal stiffness (GPa/m)	15.22	8.3	10.14	0.025
Shear stiffness (GPa/m)	6.67	3.64	4.45	0.0089
Spacing (m)	18	33	27	5
Dilatancy angle (°)	0	0	0	0

Table 5 Rating adjustments for various discontinuity orientations (Romana 1991)

Condition	Very favorable	Favorable	Fair	Unfavorable	Very unfavorable
Rating adjustment	0	-5	-25	-50	-60

Hosseinzadeh 2015; Sarkar et al. 2012) and landslides assessment (Qi et al. 2016) throughout the world. The SMR method is appropriate for the evaluation of the slope stability and can provides corresponding support. The related parameters considering discontinuities conditions, excavation condition, and the failure modes, are included in the risk assessment of the slope.

The failure modes of the soil slope and rock slope determine the classification of the slope. The failure modes of the slope are always controlled by different type of discontinuities (Goel and Singh 2011). The failure mode occurred in the rock slope include the following patterns:

Plane failure: The predominant discontinuities are consistent with the slope inclination that control the stability of the slope, the failure will happen along the predominant discontinuities.

Wedge failure: The unstable wedge block that has the same dip direction with the slope occurred from the intersection of two different planes of discontinuities.

Toppling failure: The predominant discontinuities tend to be opposite to the slope tendencies have negative effect on the slope stability. The failure occurs along the predominant discontinuities.

Soil-type failure: The condition of rock mass may be heavily jointed, strong weathered or very weak rock mass. The failure of the slope may occur along an intersection joints surface.

The SMR system can be used to evaluate the risk of slope instability. Furthermore, the appropriate support methods and different instability classes were given for each SMR range according to the results for the SMR index. The SMR system considers the factors that have directly effect on the stability of the slope. It can be expressed as Eq. (1):

$$SMR = RMR + F1 \times F2 \times F3 + F4 \tag{1}$$

where *RMR* is the sum of *I*₁ to *I*₅; *F*₁ reflects the relationship between the joints dips and the slope surface; *F*₂ is relevant to effect of the joints in the planar failure mode; *F*₃ reflects the relationship of dip angle between the slope and the joints; *F*₄ is

the influence on the stability of the slope for different excavation methods. The factors can be obtained as following definition.

Tomas et al. (2007) postulated following Eq. (2) for calculating *F*₁:

$$F1 = \frac{16}{25} - \frac{3}{500} \tan^{-1} \left(\frac{1}{10} (|A| - 17) \right) \tag{2}$$

For the planar and toppling failures, *A* is the angle between the joints and the strikes of slope face (*α_j-α_s*). While for the wedge failure, *A* represent to the angle of the dip direction between the line of the intersection of the joints (*α_i*) and the slope (*α_s*). Additionally, *F*₂ is relevant to effect of the joints in the planar failure mode, and its range is from 0.15 to 1. Tomas et al. (2007) proposed the Eq. (3) for calculating *F*₂:

$$F2 = \frac{9}{16} + \frac{1}{195} \tan^{-1} \left(\frac{17}{100} B - 5 \right) \tag{3}$$

For the planar and toppling failures, *B* represents the joint dip angle (*β_j*), in degrees. For the toppling failure mode, *F*₂ remains as 1.0. While, for the wedge failure, *B* corresponds to discontinuities dip angle (*β_j*) of the intersection line. Tomas et al. (2007) also established the following equations to estimate *F*₃.

$$F3 = -30 + \frac{1}{3} \tan^{-1} (C) \tag{4}$$

$$F3 = -13 - \frac{1}{7} \tan^{-1} (C - 120) \tag{5}$$

where *C* representing the relationship of dip angles between discontinuities (*β_j*) and slope (*β_s*) which is defined as *β_j - β_s*, *β_i - β_s*, *β_j + β_s* for the plane, wedge, and toppling failure, separately. Equation (4) is employed for the plane or wedge failures of the slope, while Eq. (5) is used for the toppling failure of the slope. *F*₄ lists the adjustment factors of the excavation method as shown in Table 6.

The related parameters of the discontinuities of the south slope are achieved through digital photogrammetry technique

Table 6 Adjustment factor as a function of the method of excavation (Romana 1991)

Excavation method	Naturalslope	Pre-splitting	Smooth blasting	Normal blasting	Deficient blasting	Mechanical excavation
Adjustment factor	15	10	8	0	-8	0

Table 7 The basic condition of discontinuities

Item	Dip direction (°)	Dip (°)
Slope face	339	32
Bedding plane	339	28
Joint set J ₁	339	34
Joint set J ₂	285	52
Joint set J ₃	106	54

and field survey. According to the on-site survey and discontinuity patterns, the planar failure is easily take place in the south slope. Therefore, the planar failure is considered and the SMR method is used to assess the stability of the south slope. The weak bedding plane and predominant joint sets information of the south slope is listed in Table 7.

The excavation method in this project is the mechanical excavation and there is no blasting method employed. The bedding plane is almost parallel to the slope surface. Additionally, the weak layer with the same dip direction easily caused the evolution of planar failure. The SMR method was used to assess the stability, and adjustment factors were achieved through Eqs. 2, 3, 4 based on probabilities of the planar failure mode. Thereafter the value of SMR was achieved via Eq. (1).

After the determination of the SMR value, the slope stability can be assessed according to the different classes of stability value proposed by Romana (1991, 1995a, b) as shown in Table 8. Thereafter the appropriate support method can be found from the support system of each SMR class separately.

Numerical modeling

Since not all characteristics of the rock slope are included in the classification system, such as the mechanical parameters and the roughness of the discontinuities. Therefore, the two-dimensional numerical model was established to study the stability of the south slope of Fushun West Open-pit Mine.

In order to analyze the stability and study the deformation behavior of the south slope of the open-pit. The two-dimensional distinct numerical model was established to perform the failure process of the slope in this study as shown in

Fig. 10. The typical section I-I is selected in the west of the slope and the position is shown in Fig. 5. The dominant joint sets of both basalt and granite gneiss layer were generated based on the dip angles from the digital photogrammetry method. The bedding plane was also considered in the model. Because the layer between the bedding plane belongs to the weak layer, the properties are mainly depended on the strength of itself strength, so the joints in the layer between the bedding plane were not considered. Considering the feasible calculation of the numerical model, the spacing of the joints was increased. The rock block was assumed obey an elastic–plastic constitutive behavior and discontinuities were modeled using an elasto-plastic model with Mohr-Coulomb failure criterion.

The shear strength reduction method is included in Universal Distinct Element (UDEC), so the factor of safety can be estimated to capture the stability of the jointed slope. The UDEC supplies an automatic search for the factor of safety (FOS) of the slope using the bracketing approach and can allow us to estimate the FOS. During the calculation, the friction angle and cohesion of both the rock mass and discontinuities are reduced by a strength reduction factor. The FOS can be obtained once the numerical model cannot reach equilibrium. The FOS is regarded as the ratio of the actual shear strength of the rock mass to the reduced shear strength when it reached failure time (Wesley and Leelaratnam 2002).

Results

Evaluation of rock mass quality

The rainfall is considered as a trigger factor of slope instability of the Fushun West Open-pit Mine. The water distribution has a significant effect on the quality of the rock mass and stability of the south slope, thus, the water distribution map of the slope can be obtained by infrared scanning technique. As shown in Fig. 8, there are 6 obviously low temperature zones lies below the road III and to the east of the water pipeline. The low temperature zone is delineated in the figure. Above the road III, there are two vertical low temperature bands named bands 7 and 8 delineated in the Fig. 8. Through field surveying, it can be found that bands 7 and 8 are large water discharge areas

Table 8 The description of SMR grading

Class No.	Grade	Stability	Failure modes	Reinforcement
V	0~20	Very bad	Large planar or soil-like	Re-excavation
IV	21~40	Bad	Planar or big wedges	Strong / redesign
III	41~60	Normal	Some joints or many wedges	Systematic
II	61~80	Good	Some blocks	Local
I	81~100	Very good	None	None

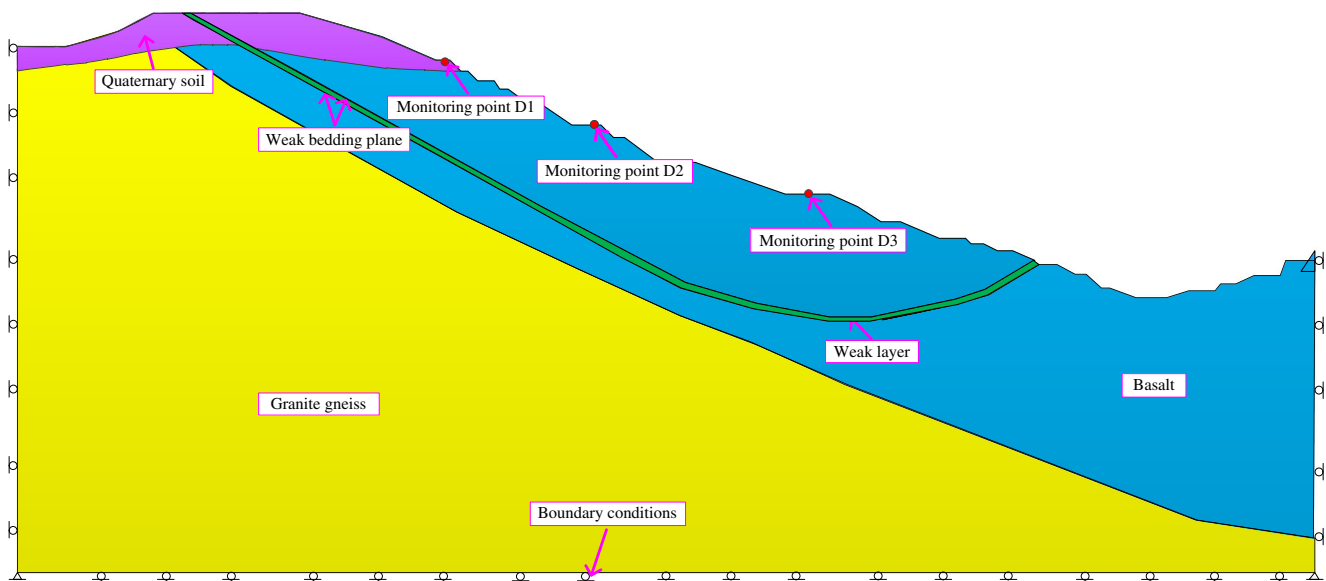


Fig. 10 The geology condition of section I-I

which are relatively wide and the amount is concentrated. Additionally, the location close to the top of the slope at elevation 30, a large area of significant low temperature can be found, the temperature in this area is lower than the surrounding rock temperature about 6~8 °C. The existence of seepage area will heavily affect the strength of the rock mass and the stability of the slope.

The quality of the rock mass was evaluated by classification system considering the detailed structure features. The result of RMR value is 60 to 65 as listed in Table 9. According to the grade description of reference Bieniawski et al (1973), the results indicate that the rock mass belongs to grade III and the quality of the rock mass tend to be partially stable.

Figure 7 shows the borehole testing result near the section I-I at the top of the south slope. The depth of the hole is 40.0 m. Due to the surface of the slope is covered by the quaternary soil, so the borehole 0~5 m is protected by the steel pipe in order to reduce the risk of the collapse of the borehole. Therefore, Fig. 7 only shows the image from 5.0 to 40.0 m. The 14.7~31.0 m is mixed with the coal seam and the fissure zones. The cracks and breakdown areas can be observed at 8.4 m, 14.8~15.8 m, 17.4~19.9 m, 22.9~24.8 m, 25.7 m, 26.2 m, 28.6~30.4 m, 26.2 m, 28.6~30.4 m, and 30.8 m. The region between 33.0 and 34.5 m has some large fissures. From 34.5 to 35.3 m some opening fissures can be found in this region.

While in the region 36.5~40.0 m the broken zones can be clearly identified. From the monitoring result of the borehole TV technique, the fissure zones, and broken areas can be clearly identified in the slope. The coal seam and the carbonaceous mudstone mixed can also be observed in the slope. However, the fissure zone and the broken zone are small and the broken zone is not totally ruptured. At the same time, there is no obvious water leakage in the borehole. The interior rock mass quality of the south slope can be visualized through the borehole TV technique. The rock mass of the slope is partially stable in general. This is almost in accordance with the estimation of the RMR results.

Evaluation of SMR values

The detail of the adjustment factors and the result of the SMR are presented in Table 10. The minimum estimation result of SMR (SMR=32.9) was regarded as the stability assessment value, which is obtained on the basis of the adjustment factors for the weak layer. The result of the SMR indicates that the planar failure along the bedding plane probably occurred in the south slope. The slope may slide along the bedding planes. The result of critical SMR value (SMR=32.9) of the south slope belongs to class IV, meaning unstable conditions. Thus, it is necessary to strongly reinforced or redesigned the slope. The damage in situ also revealed some characteristics of

Table 9 The evaluation of the quality of the rock mass

Item	UCS (MPa)	RQD	Space of discontinues	The condition of discontinues	The condition of groundwater	RMR value
Value/description	52-60	55	0.4-1.1	Strong weathered	Dry to damp joints	
Rating value	7	13	10-15	20	10	60-65

Table 10 Adjustment factors and the SMR value

	F_1	F_2	F_3	F_4	$F_1 * F_2 * F_3 + F_4$	SMR
The bedding and slope face	1	0.49	-55.32	0	-27.1	32.9
The joint J_1 and slope face	1	0.76	-8.86	0	-6.7	53.3
The joint J_2 and slope face	0.64	0.95	-0.95	0	-0.58	59.4
The joint J_3 and slope face	0.64	0.96	-0.87	0	-0.53	59.5
Critical SMR value	32.9					

the planar failure of the south slope and the SMR results are consistent with the field observations.

Evaluation of numerical modeling

The results of the typical section of the south slope are presented in Fig. 11. The vector of the velocity clearly indicates the landslide of the slope mainly occurred along the weak bedding plane. It indicates that the block near the bedding plane changing fast and the block near the slope surface are slow down. Figure 11(b) also shows the failure mode of the slope when the FOS is 1.09 approximately to 1.0. The FOS of the slope indicates that the slope is in limit equilibrium state. The displacement in X direction is obvious in the toe of the slope and the top of the slope. The X-displacement in the deep of the slope along the weak bedding plane means that the landslide is mainly slip along the bedding plane. Figure 11(c) shows the major stress contour of the slope, the stress distribution is relatively uniform, only a small part of the stress concentrated near some joint sets and weak layer. The result in Fig. 11(d) also illustrates that the planar failure is the primary failure mode of the south slope. The displacement near the slope surface is relative small indicates that the joint sets are the secondary factor for the triggering of landslide in the south slope. However, it should note that the combination of joint sets in the frontal surfaces may form some isolated blocks and detach from the slope.

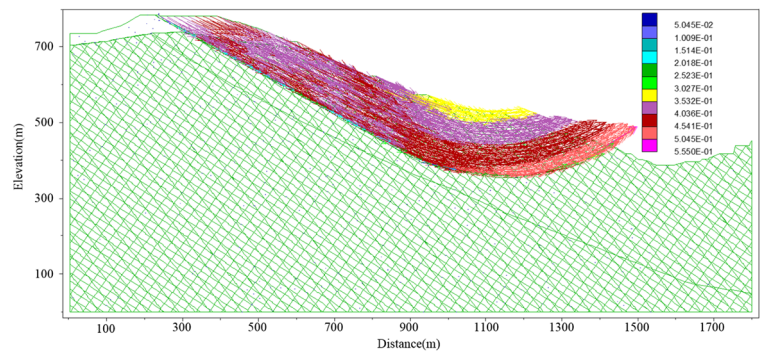
From the deformation phenomenon on site and the numerical simulation analysis, it is known that the slope is already in the state of limit equilibrium. In order to prevent further deformation of the slope, the backfill presser foot method was proposed to increase the anti-sliding force of the slope. Due to the large amount of the pressing foot project, the mine carried out the backfill work in three stages, and the pressing foot work continued until the end of June 2014. In order to evaluate the effect of the pressing foot project, the 2D numerical model after the pressing foot of the slope based on discrete element method was established.

The slope after the reinforcement is simulated and the effects are analyzed. The result of the simulation is presented in Fig. 12. It is clearly shown that the velocity of the block is reduced and the direction of the block is changed to the downward and this is beneficial to the stability of the slope. The

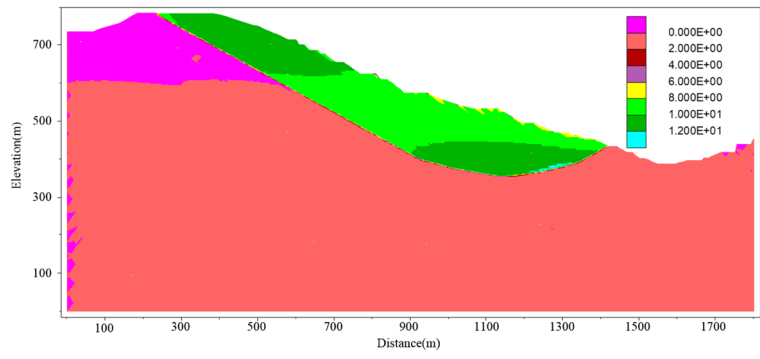
instability trend of the slope has been obviously suppressed. Only a little part of the block on the surface of the slope still has large deformation, the overall stability of the slope has been greatly improved, and the FOS of the slope has risen to 1.41. The displacement in X direction illustrates that the displacement is obviously decreased due to the reinforcement of the slope. The decreasing of displacement in X direction reveals that the reinforcement of the slope achieved a good result (Fig. 12(b)). The shear stress and compressive stress concentration is occurred in the toe of the slope demonstrate that the pressing foot project has effectively prevent further sliding of the slope (Fig. 12(c)).

In order to further acquire the deformation characteristics of the slope, the monitoring point D1, D2, and D3 (Fig. 10) were selected to analyze the damage process of the slope. The monitoring data curve of monitoring point D1, D2, and D3 from April 25, 2013 to October 2, 2014 is presented in Fig. 9. It is shown that in Fig. 9(a) the deformation rate gradually increased from 2013, especially from August 2013 due to the rainy season. After that, there was a brief decrease, and then the deformation rate began to increase rapidly again. This was mainly because the slope was already in the state of limit equilibrium. But after the implementation of the pressing foot project, the slope deformation rate has decreased significantly. The curve of monitoring point D2 shows a similar law with D1, but the deformation rate is not decreased in November 2013 and the value is relatively small than monitoring point D1 (Fig. 9(b)). The law of monitoring point D3 is roughly the same with monitoring point D1 and the value of the deformation rate is the lowest of three monitoring points (Fig. 9(c)). It is also shown that without the pressing foot of the south slope, the deformation rate is relative large. The maximum displacement of D1, D2, and D3 was 170 mm, 144 mm, and 56 mm separately for each day. While in the case after the pressing foot of the slope, the maximum deformation of D1, D2, and D3 was reduced to 101 mm, 69 mm, and 16 mm per day separately. The tendency of deformation rate decreases obviously. The deformation rate monitored on-site indicates that the pressing foot of the south slope obviously controlled the deformation of the slope along the weak bedding planes.

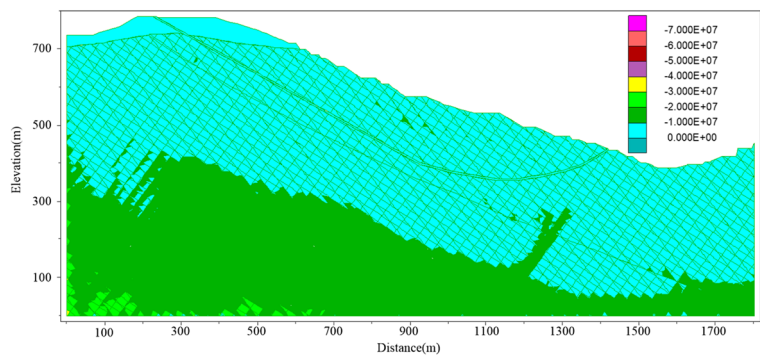
Due to the negative impact on the rock mass strength and slope stability, the water distribution map of the south slope is obtained by infrared scanning technique. According to water



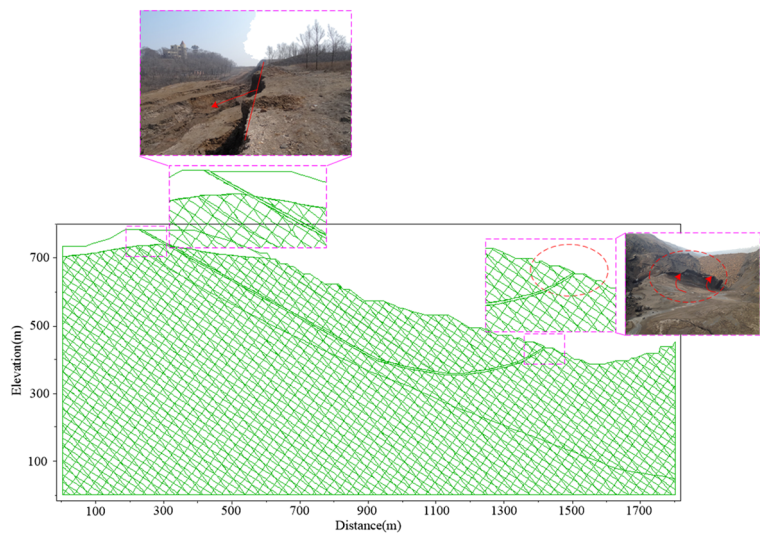
(a) the velocity vectors



(b) the X displacement contours

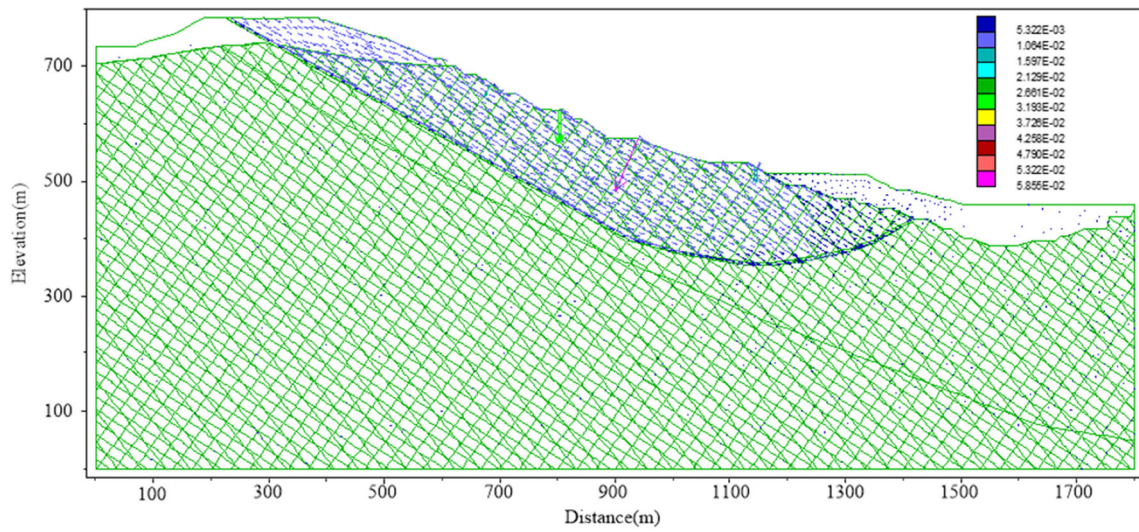


(c) the major principle stress contours

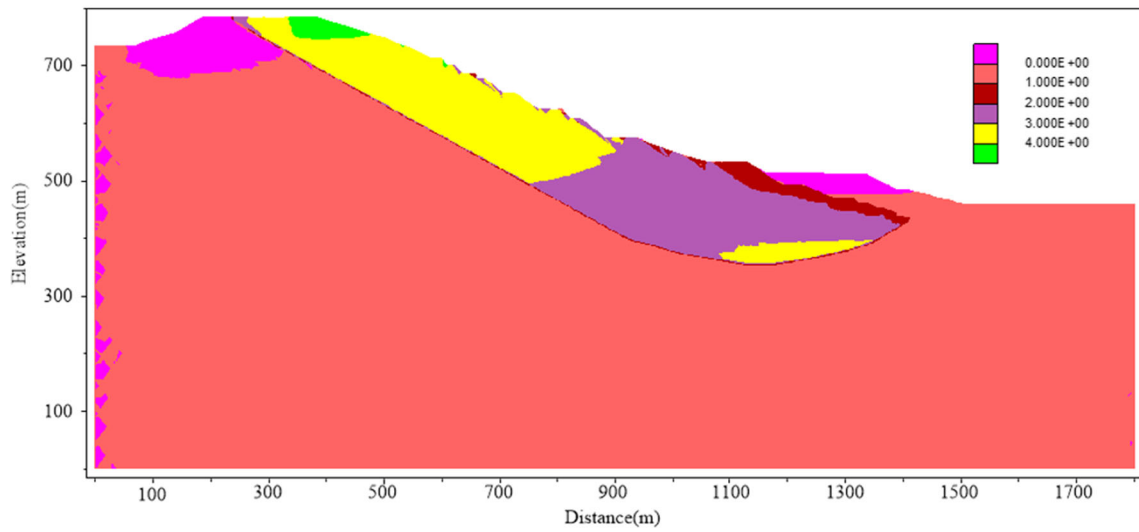


(d) the deformation of the block

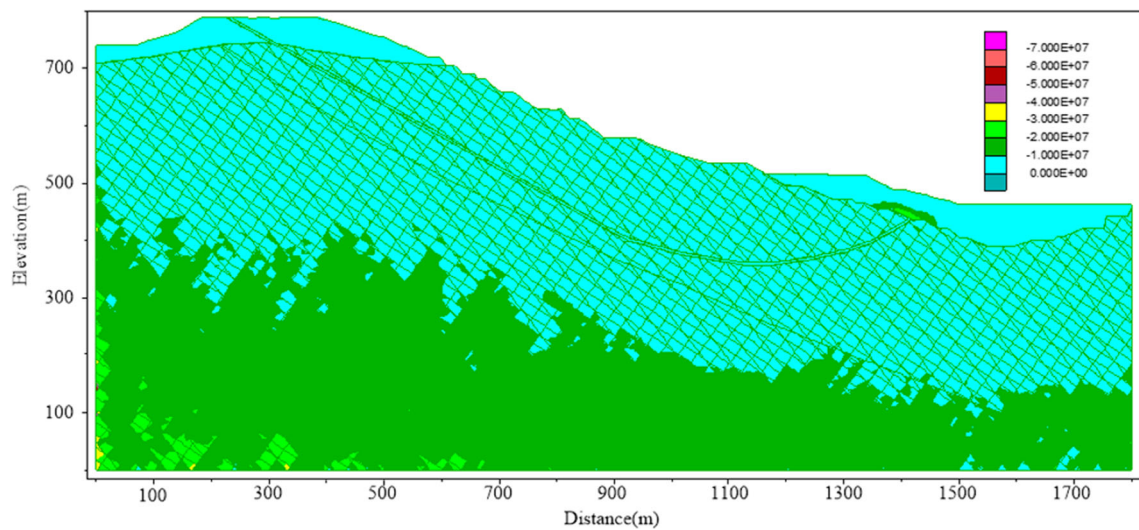
Fig. 11 The result of the numerical simulation



(a) the velocity vectors



(b) the X displacement contours



(c) the major principle stress contours

Fig. 12. The numerical result after the pressing foot of the slope

distribution map, the water leakage points and strips were delineated and the corresponding drainage system was established. The drainage ditch was employed in the place corresponding to the water leakage points and strips. Finally, the water is discharged through the pump station. The plan view of the designed drainage system is presented in Fig. 13. The construction of drainage system can further effectively control the occurrence of slope hazards.

Discussions

For the stability of complex rock slopes, the progressive research method can be used to explore its failure mechanism. The accuracy of slope stability analysis results is mostly based on some field data, including the basic characteristics of rock mass, the characteristics of structural plane, and the water conditions of slope. The numerical method further reveals failure behavior and deformation mechanism of the slope. The integration application of these data and methods add the novelty of the approach to reveal the stability of the rock slope in complex regions.

The accuracy of the related figures and data

The accuracy of joint parameters

In most cases, the stability of rock slope is closely related to the distribution and characteristics of joints. The accuracy of joint parameters directly affected the assessment result of the stability of rock slope. Nevertheless the joint parameters relates mainly to the accuracy of data, distribution, and the number of measuring sites. The digital photogrammetry technology is a technique which can obtain the joint characteristics of large area quickly. The advanced ShapeMetrix3D system has been widely used in the acquisition of the joint parameters of

rock slope, and achieved good results (Wang et al. 2018; Manzoor et al. 2020). In this study, Three different regions in the south slope were selected which covering the large deformation area of the south slope. In each area, the location where the joints fully developed should be selected for measurement. At the same time, the measurement sites should be dispersed as far as possible, so as to describe the overall development of the joints of the slope rock mass. In the field measurement, the measurement points should also be located in the area which is easy to measure. According to the above principles, three different regions totally 9 sites were measured in researched area and the joint characteristics of slope rock mass were accurately obtained. The detailed joint parameters of rock mass were processed and the results are shown in Table 1. Furthermore, the dominant joint sets were obtained, and they can also found in situ as shown in Fig. 6.

The accuracy of interior structure map of the rock mass

The borehole TV technique is used to acquire the internal structure of the rock mass. It realizes the two-dimensional representation of 360 ° borehole wall. The borehole image can directly reflect the geological characteristics in the borehole. Through the extraction and storage of the whole borehole geological information, a complete information database is formed, which can accurately evaluate the integrity of rock mass and comprehensively analyze the structural characteristics of the rock mass. In this study, four measuring sites on the top in the southwest of the slope were selected to investigate the internal structures of the rock mass. The internal structure of slope rock mass is measured near the large deformation area in west region of the south slope of the open-pit. More boreholes may increase the accuracy of understanding the underground structure in different areas of the slope rock mass, but it increases the cost and spends a lot of time. Furthermore, due to the complexity of rock mass structure in practical

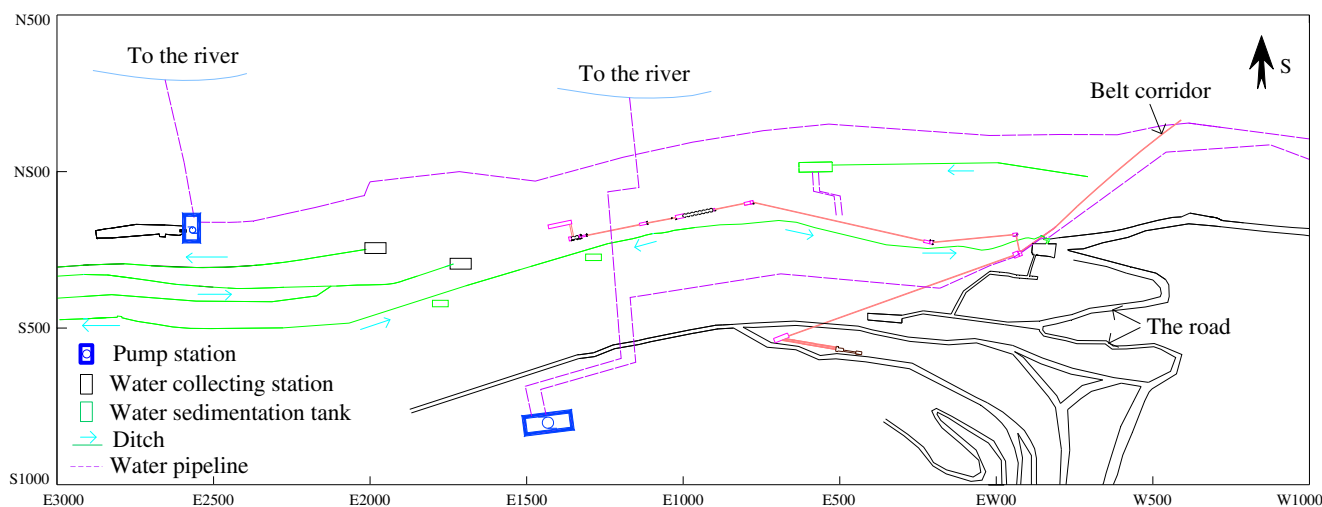


Fig. 13 The designed drainage system of the south slope of the open-pit

engineering and the continuous deformation of slope, more boreholes located on or far away from the slope deformation areas may not be able to truly reflect the original structural characteristics of the rock mass. However, the rock mass in boreholes outside the large deformation area near the deformation zone can better reflect the original structural characteristics of slope rock mass.

The accuracy of the in situ monitoring data

The GPS monitoring sites were selected in the areas with large deformation. The monitoring points were located in the back edge, middle and front edge of the slope, which can accurately capture the deformation characteristics of the slope. The in situ monitoring data are consistent with the actual deformation characteristics of the slope which proves the accuracy of the field monitoring data.

The accuracy of the water distribution map

The distribution of the water leakage points were obtained by the infrared scanning technique. In order to verify the accuracy of the monitoring result, some detailed field surveys were done. From the field survey, the water leakage positions were found on-site, as shown in Fig. 8. According to the field investigation and geological data, the source of groundwater in the slope is also revealed. The water leakage strips of 7 and 8 are large water discharge areas due to the existence of the Liushan old river. The river bedrock is undercut and the river pebble layer has good permeability, which is the channel for phreatic water to converge into the slope. At the same time, the atmospheric rainfall and surface water infiltrate into the bedrock of the slope and discharge on the surface of the slope, which indicates that there is a certain buried groundwater level in the slope. This situation is not conducive to the stability of the slope. According to the field survey on the location of the water outlet and the revelation of the groundwater source of the slope, the accuracy of the water leakage distribution map is verified.

Numerical modeling and its validation

The validation of the numerical calculation for the study of slope deformation mechanism can be verified by the monitoring data from the study area. In order to illustrate the reliability of the calculation results in this paper, three different monitoring points are selected from section I-I accordingly. Furthermore, the accumulated displacements of 3 months before and after the pressing foot project (July 1, 2014) were counted. Thereafter, both the numerical monitoring data and the corresponding in situ monitoring data were presented in Fig. 14. It indicates that the displacement decreased with the pressing foot project and the displacement of the slope

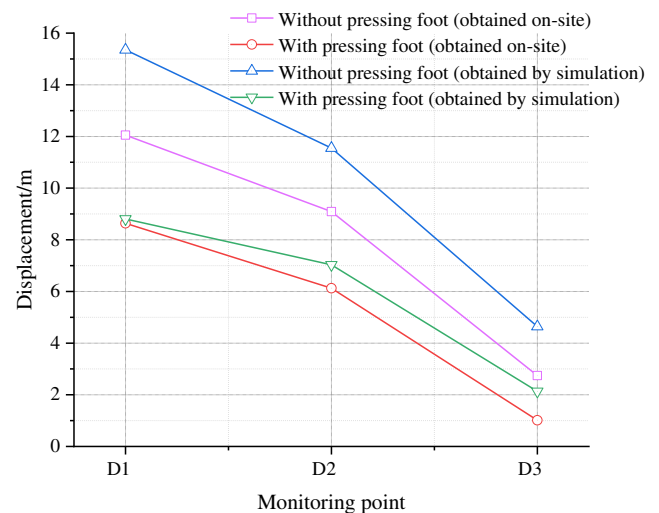


Fig. 14 The displacement curve without and with pressing foot of the south slope

gradually decreases from top to bottom. The tendency of on-site monitoring data is consistent with the simulation results. The damage zone delineated by the simulation can also observe in situ (Fig. 11(d)). The simulation can reproduce the failure process of the south slope and forecast the possibly deformation trend. The numerical results also reveal the same failure mode with the empirical method. Both the empirical method and numerical method reveal that the weak bedding plane is the main factor leading to the instability of the slope.

Some geological disasters often occur in complex rock slopes. It is difficult to observe the deformation process and the internal stress distribution characteristics of the slope directly. With the help of numerical calculation, the deformation process of the slope can be well reproduced and the internal stress distribution characteristics of the slope can be mastered. At the same time, the possible failure mode and damage zone can be identified and delineated. According to the calculation results, the detailed reinforcement scheme can be formulated, and the reinforcement effect and subsequent deformation trend can also be evaluated. This outcome will assist the decision-makers to understand deeper insight into the deformation mechanism and failure process. It can also help them make a detailed reinforcement scheme to prevent further deformation of the slope and evaluate the reinforcement effect.

Conclusions

A progressive method was utilized to estimate the stability of the rock slope under complex geological conditions in Fushun West Open-pit Mine, some conclusions can be drawn:

- (1) The rock mass quality in the south slope of the open-pit was evaluated by the rock mass classification system. The rock layer is belonging to grade III of partially

stable. The borehole TV technique is utilized to acquire the interior quality of the rock mass. It is shown that the rock mass have some fissure zones and broken areas, the rock mass tend to be stable overall.

- (2) The modified SMR system was used to predict the stability of the south slope in the open-pit. The result of the SMR reports that the discontinuities have great impact on the stability of the slope. The result shows that the planar failure is easily occurred in the slope particularly for the bedding plane causing the instability of the slope.
- (3) Due to the associated classification systems not considering the detailed condition of the slope, the numerical method is used to study the stability of the slope. The result shows that the discontinuities have the significant effect for the instability of the slope especially for the bedding plane. The numerical result is in acceptable accordance with the SMR result. The validation of the numerical result can be vilified by the in situ monitoring data. According to the estimation of the stability of the slope, the targeted management method is proposed. The pressing foot project can prevent further deformation of the slope and the infrared scanning technique can provide a reference for the establishment of the drainage system in order to enhance the strength of the weak layer and rock mass.
- (4) This study provides a promising method to help the decision makers to identify potentially dangerous slopes in the early stages and deeply understand the deformation mechanism of the slope. Additionally, different measures should be taken in time according to the analysis results to reduce the possible hazards especially for the excavated rock slope.

Acknowledgements The research content in this article was finally supported by the National Key Research and Development Program of China (Grant No. 2017YFC1503101), National Natural Science Foundation of China (NSFC) under grant No. 51978426. We thank Mr. Jian-li Cao for providing the help of Borehole TV technique and Prof. Shan-jun Liu for the infrared scanning interpretation. We are also grateful for the support of Fushun West Open-pit Mine in the aspect of field investigation. We are also grateful to the anonymous reviewers for their valuable comments, which have greatly improved this paper.

Declarations

Competing interests The authors declare no competing interests.

References

Abuzied SM, Alrefae HA (2019) Spatial prediction of landslide-susceptible zones in El-Qaá area, Egypt, using an integrated approach based on GIS statistical analysis [J]. *Bull Eng Geol*

- Environ* 78(4):2169–2195. <https://doi.org/10.1007/s10064-018-1302-x>
- Abuzied SM, Pradhan B (2020) Hydro-geomorphic assessment of erosion intensity and sediment yield initiated debris-flow hazards at Wadi Dahab Watershed, Egypt[J]. *Georisk Assess Manage Risk Eng Syst Geohazards*:1–26. <https://doi.org/10.1080/17499518.2020.1753781>
- Abuzied S, Ibrahim S, Kaiser M, Saleem T (2016) Geospatial susceptibility mapping of earthquake-induced landslides in Nuweiba area, Gulf of Aqaba, Egypt[J]. *J Mt Sci* 13(7):1286–1303. <https://doi.org/10.1007/s11629-015-3441-x>
- Barton N, Lien R, Lunde J (1974) Engineering classification of masses for the design of tunnel support. *Rock Mech* 6(4):189–236
- Bhasin R, Pabst T (2015) Finite element and distinct element analysis of the stability of a large underground hydropower machine hall in the Himalayas [J]. *KSCE J Civ Eng* 19(3):725–732
- Bieniawski ZT (1973) Engineering classification of jointed rock masses [J]. *Civil Eng South Africa* 1973(12): 335–343
- Bieniawski ZT (1989) Engineering rock mass classifications: a complete manual for engineers and geologists in mining, civil, and petroleum engineering [M]. John Wiley & Sons, New York
- CCTEG (2013). Shenyang research Institute. Investigation on the stability of south slope of Fushun West Open-pit Mine [R]. Fushun: CCTEG Shenyang research Institute, :1-94. (in Chinese)
- Chen YF, Zheng HK, Wang M, Hong JM, Zhou CB (2015) Excavation-induced relaxation effects and hydraulic conductivity variations in the surrounding rocks of a large-scale underground powerhouse cavern system [J]. *Tunn Undergr Space Technol* 49:253–267. <https://doi.org/10.1016/j.tust.2015.05.007>
- Chigira M, Hariyama T, Yamasaki S (2013) Development of deep-seated gravitational slope deformation on a shale dip-slope: observations from high-quality drill cores [J]. *Tectonophysics* 605:104–113. <https://doi.org/10.1016/j.tecto.2013.04.019>
- Crozier MJ (1986) Landslides: causes, consequences & environment [M]. Taylor & Francis, London
- Farahmand K, Diederichs MS (2021) Calibration of coupled hydro-mechanical properties of grain-based model for simulating fracture process and associated pore pressure evolution in excavation damage zone around deep tunnels [J]. *J Rock Mech Geotech Eng* 13(1): 60–83. <https://doi.org/10.1016/j.jrmge.2020.06.006>
- Goel RK, Singh B (2011) Engineering rock mass classification: tunneling, foundations and landslides [M]. Butterworth-Heinemann, Boston
- He S, Li Y, Aydin A (2018) A comparative study of UDEC simulations of an unsupported rock tunnel [J]. *Tunn Undergr Space Technol* 72: 242–249. <https://doi.org/10.1016/j.tust.2017.11.031>
- Hoek E, Kaiser PK, Bawden WF (2000) Support of underground excavations in hard rock [M]. CRC Press, London
- Huang J, Sun C, Wu X, Ling S, Wang S, Deng R (2020) Stability assessment of tunnel slopes along the Dujiangyan City to Siguniang Mountain Railway, China [J]. *Bull Eng Geol Environ* 79(10): 5309–5327. <https://doi.org/10.1007/s10064-020-01913-9>
- Itasca (2004) UDEC: Universal Distinct Element Code, version 4.0. Itasca Inc., Minneapolis.
- Kalililo M, Xia Y (2020) UDEC-based stability analysis of jointed bedding slope and slope parameter optimization suggestions: a case study [J]. *SN Appl Sci* 2(12):1–21. <https://doi.org/10.1007/s42452-020-03748-1>
- Laubscher DH (1990) A geomechanics classification system for the rating of rock mass in mine design [J]. *J South Afr Inst Min Metall* 90(10):257–273
- Liu S, Dai S, Li W, Han B, He B, Luo J (2020) A new monitoring method for overlying strata failure height in Neogene laterite caused by underground coal mining [J]. *Eng Fail Anal* 117:104796. <https://doi.org/10.1016/j.engfailanal.2020.104796>

- Manzoor S, Liaghat S, Gustafson A, Johansson D, Schunnesson H (2020) Establishing relationships between structural data from close-range terrestrial digital photogrammetry and measurement while drilling data [J]. *Eng Geol* 267:105480. <https://doi.org/10.1016/j.enggeo.2020.105480>
- Pantelidis L (2009) Rock slope stability assessment through rock mass classification systems [J]. *Int J Rock Mech Min Sci* 46(2):315–325. <https://doi.org/10.1016/j.ijrmmms.2008.06.003>
- Pantelidis L (2010) An alternative rock mass classification system for rock slopes [J]. *Bull Eng Geol Environ* 69(1):29–39. <https://doi.org/10.1007/s10064-009-0241-y>
- Pinheiro AL, Lana MS, Sobreira FG (2015) Use of the distinct element method to study flexural toppling at the Pico Mine, Brazil [J]. *Bull Eng Geol Environ* 74(4):1177–1186. <https://doi.org/10.1007/s10064-014-0713-6>
- Qi C, Wu J, Liu J, Kanungo DP (2016) Assessment of complex rock slope stability at Xiari, southwestern China [J]. *Bull Eng Geol Environ* 75(2):537–550. <https://doi.org/10.1007/s10064-015-0763-4>
- Romana M (1991). SMR classification [C]//7th ISRM Congress. International Society for Rock Mechanics.
- Romana M (1995a). A geomechanical classification for slopes: slope mass rating [M]//Rock Testing and Site Characterization.
- Romana M (1995b). The geomechanical classification SMR for slope correction [C]//8th ISRM Congress. International Society for Rock Mechanics: 575–600.
- Rusdy I, Fathani TF, Al-Huda N, Iqbal K, Jamaluddin K, Meilianda E (2021) Integrated approach in studying rock and soil slope stability in a tropical and active tectonic country [J]. *Environ Earth Sci* 80(2): 1–20. <https://doi.org/10.1007/s12665-020-09357-w>
- Salmi EF, Hosseinzadeh S (2015) Slope stability assessment using both empirical and numerical methods: a case study [J]. *Bull Eng Geol Environ* 74(1):13–25. <https://doi.org/10.1007/s10064-013-0565-5>
- Santos A, Lana MS, Pereira TM (2020) Rock Mass Classification by Multivariate Statistical Techniques and Artificial Intelligence [J]. *Geotech Geol Eng* 12:1–22. <https://doi.org/10.1007/s10706-020-01635-5>
- Sarkar S, Kanungo DP, Kumar S (2012) Rock mass classification and slope stability assessment of road cut slopes in Garhwal Himalaya, India [J]. *Geotech Geol Eng* 30(4):827–840. <https://doi.org/10.1007/s10706-012-9501-x>
- Singh HO, Ansari TA, Singh TN, Singh KH (2020) Analytical and numerical stability analysis of road cut slopes in Garhwal Himalaya, India [J]. *Geotech Geol Eng* 38(5):4811–4829. <https://doi.org/10.1007/s10706-020-01329-y>
- Tizzano A, Shakoor A, Lund WR (2016) Characterization of failure parameters and preliminary slope stability analysis of the Cedar Canyon Landslide, Iron County, Utah [J]. *Environ Eng Geosci* 22(3):245–258. <https://doi.org/10.2113/gsegeosci.22.3.245>
- Tomas R, Delgado J, Seron J B (2007). Visual sensibility analysis of slope mass rating (SMR) correction parameters using continuous functions [C]//11th ISRM Congress. International Society for Rock Mechanics.
- Wang PT, Yang TH, Xu T, Yu QL, Liu HL (2013) A model of anisotropic property of seepage and stress for jointed rock mass. *J Appl Math* 2013:361–376. <https://doi.org/10.1155/2013/420536>
- Wang F, Wang S, Hashmi MZ, Xiu Z (2018) The characterization of rock slope stability using key blocks within the framework of GeoSMA-3D [J]. *Bull Eng Geol Environ* 77(4):1405–1420. <https://doi.org/10.1007/s10064-018-1291-9>
- Wesley LD, Leelaratanam V (2002) Shear strength parameters from back-analysis of single slips [J]. *Geotechnique* 52(6):463–464. <https://doi.org/10.1680/geot.52.6.463.38744>
- Wickham GE, Tiedemann HR, Skinner EH (1972). Support determination based on geologic predictions. In: Lane KS, Garfield LA (eds) *Proceedings of the North American Rapid Excavation Tunneling Conference (RETC)*, Chicago. Society for Mining, Metallurgy, and Exploration, American Institute of Mining, Metallurgical and Petroleum Engineers (AIME), New York, pp 43–64.
- Yang TH, Xie LK, Wang SY, Zheng H, Rui YQ, Tang CA (2005) Effect evaluation of distribution for north project of side slope in Fushun west open cast [J]. *Chin J Rock Mech Eng* 24(11):1841–1846 (in Chinese)
- Yang TH, Wang PT, Xu T, Yu QL, Zhang PH, Shi WH, Hu GJ (2015) Anisotropic characteristics of jointed rock mass: a case study at Shirengou iron ore mine in China [J]. *Tunn Undergr Space Technol* 48:129–139. <https://doi.org/10.1016/j.tust.2015.03.005>
- Zhang ZL, Liu G, Wu SR, Tang HM, Wang T, Li GY, Liang CY (2015) Rock slope deformation mechanism in the Cihaxia Hydropower Station, Northwest China [J]. *Bull Eng Geol Environ* 74(3):943–958. <https://doi.org/10.1007/s10064-014-0672-y>
- Zhang F, Yang TH, Li LC, Wang Z, Xiao P (2019) Cooperative monitoring and numerical investigation on the stability of the south slope of the Fushun west open-pit mine [J]. *Bull Eng Geol Environ* 78(4): 2409–2429. <https://doi.org/10.1007/s10064-018-1248-z>
- Zhao L, Yu C, Cheng X, Zuo S, Jiao K (2020) A method for seismic stability analysis of jointed rock slopes using Barton-Bandis failure criterion [J]. *Int J Rock Mech Min Sci* 136:104487. <https://doi.org/10.1016/j.ijrmmms.2020.104487>
- Zheng Y, Chen C, Liu T et al (2018) Study on the mechanisms of flexural toppling failure in anti-inclined rock slopes using numerical and limit equilibrium models [J]. *Eng Geol* 237:116–128. <https://doi.org/10.1016/j.enggeo.2018.02.006>